



## Article

# Paving the Way for Last-Mile Delivery in Greece: Data-Driven Performance Analysis with a Customized Quadrotor

Charalabos Ioannidis, Argyro-Maria Boutsis \*, Georgios Tsingenopoulos, Sofia Soile , Regina Chliverou and Chryssy Potsiou

Laboratory of Photogrammetry, School of Rural, Surveying and Geoinformatics Engineering, National Technical University of Athens, 15773 Athens, Greece; cioannid@survey.ntua.gr (C.I.); georgetsig@central.ntua.gr (G.T.); ssoile@survey.ntua.gr (S.S.); regina@survey.ntua.gr (R.C.); chryssyp@survey.ntua.gr (C.P.)

\* Correspondence: iboutsis@mail.ntua.gr

**Abstract:** Cargo drones are a cutting-edge solution that is becoming increasingly popular as flight times extend and regulatory frameworks evolve to accommodate new delivery methods. The aim of this paper was to comprehensively understand cargo drone dynamics and guide their effective deployment in Greece. A 5 kg payload quadrotor with versatile loading mechanisms, including a cable-suspended system and an ultra-light box, was manufactured and tested in five Greek cities. A comprehensive performance evaluation and analysis of flight range, energy consumption, altitude-related data accuracy, cost-effectiveness, and environmental were conducted. Based on hands-on experimentation and real-world data collection, the study proposes a novel data-driven methodology for strategically locating charging stations and addressing uncertainties like weather conditions and battery discharge during flights. Results indicate significant operational cost savings (89.44%) and a maximum emissions reduction (77.42%) compared to conventional transportation. The proposed strategic placement of charging stations led to substantial reductions in travel distance (41.03%) and energy consumption (56.73%) across five case studies in Greek cities.

**Keywords:** cargo drone; drone-based logistics; drone routing; charging stations; GIS



**Citation:** Ioannidis, C.; Boutsis, A.-M.; Tsingenopoulos, G.; Soile, S.; Chliverou, R.; Potsiou, C. Paving the Way for Last-Mile Delivery in Greece: Data-Driven Performance Analysis with a Customized Quadrotor. *Drones* **2024**, *8*, 6. <https://doi.org/10.3390/drones8010006>

Academic Editor:  
Pablo Rodríguez-González

Received: 9 November 2023  
Revised: 20 December 2023  
Accepted: 27 December 2023  
Published: 29 December 2023



**Copyright:** © 2023 by the authors. Licensee MDPI, Basel, Switzerland. This article is an open access article distributed under the terms and conditions of the Creative Commons Attribution (CC BY) license (<https://creativecommons.org/licenses/by/4.0/>).

## 1. Introduction

Unmanned aerial vehicles (UAVs), commonly known as drones, are transforming into multifunctional platforms for several intricate tasks. Equipped with advanced GPS systems and multispectral sensors, they are capable of autonomous flight, precision navigation, and high-resolution sensing. Thus, drones showcase their versatility across multiple sectors, including agriculture, environmental monitoring, surveying, defense, cinematography, archaeology, etc. An unexplored and intriguing area of application is logistics. Their integration into last mile delivery introduces the term “Cargo drones”. Drones are exploited at the final stage of a product’s journey from a distribution center or warehouse to its ultimate destination, which is often a customer’s doorstep or a retail store. In Greece, traditional road transport has been the primary delivery method for many years. Cargo drones could excel in the last mile supply chain, especially in densely populated urban areas where traffic congestion impedes vans and trucks. The development of appropriate infrastructure, such as charging stations and landing zones, could lead to lower operational costs in terms of labor, fuel, and maintenance expenses associated with conventional modes of transportation. The Hellenic Civil Aviation Authority categorizes drone regulations based on their weight and intended operation. Based on the European Aviation Safety Agency (EASA, Cologne, Germany), urban operations on logistics are treated as ‘specific operations’ and the applicable requirements are based on the results of a risk assessment [1]. However, a national regulatory framework for cargo drones is nonexistent. Besides regulatory and legal hurdles, introducing cargo drones into the logistics landscape of Greece requires extensive

performance analysis and terrain-aware planning due to the diversity of the land cover and relief. Relative research either tends to focus on flight simulations or make idealized assumptions about the design of the cargo drones.

This work offers practical guidance for the ongoing development and deployment of this innovative aerial delivery solution in Greece, where drone deliveries remain an underdeveloped field of logistics. A custom-made quadrotor was designed, assembled, and tested under a variety of real-world circumstances, including parcel weights, weather conditions, altitude profiles, delivery distances, and land uses. It followed established paths to reach designated destinations in five Greek cities, Athens, Korinthos, Patra, Kalamata, and Iraklion. It incorporated two delivery mechanisms for precise control over its positioning and altitude to deliver safely and unload parcels automatically. The extensive data comprising 58 distinct delivery cases that reflect its real-world performance under different operational constraints were gathered, processed, and analyzed. The computation of the energy consumption patterns accounted for the impact of load changes and hovering on the quadrotor's energy utilization. Moreover, an altimetric accuracy assessment of the shuttle radar topography mission (SRTM) [2] of Mission Planner software [3] at the regional level was performed, while operational cost was calculated, compared to conventional modes of transportation. The contributions of this work are summarized as follows:

- The design, manufacturing, and semi-autonomous flight testing were conducted using a customized quadrotor of 5 kg payload capacity that supports the following two types of loading–unloading mechanisms: suspended beneath by a cable with auto-retraction or stored in an ultra-light box, attached to the multirotor body.
- Data-driven methodology was used for charging stations for cargo shipping, while also taking in uncertainties encountered during the flight, such as weather conditions and battery discharge.
- The following were conducted performance evaluation of flight range and energy consumption, cost-benefit analysis compared to a conventional delivery van, and the altimetric assessment of SRTM Digital Terrain Elevation Data (DTED) for systematic errors at a local and regional base in Greece.

The remainder of this paper is organized as follows. Section 2 provides a detailed review of research, focusing on prominent last-mile delivery cases, performance analysis methods, and routing optimization plans. Section 3 details the specifications and variants of the prototype cargo drone. It presents the design parameters, the mechanical and computational components, as well as the safety mechanisms of the developed platform. Section 4 outlines the methodological approach, involving the performance equations that address the charging station's problem. Section 5 presents the case studies, examines the performance, and discusses the analysis results, and finally, Section 6 concludes the research and proposes future work.

## 2. Literature Review

### 2.1. State of Cargo Drone Operations

Numerous initiatives, projects, and applications in the field of cargo drones have demonstrated their ability to serve diverse logistics needs in retail, healthcare, humanitarian aid, and disaster relief. Regarding commercial endeavors, the first drone deliveries were introduced by Amazon Inc. under the service Amazon Prime Air [4], while the global logistics and courier delivery company DHL designed PaketKopter for light-weight packages and 12 km flight ranges [5]. Wingcopter was founded in 2017 and integrated cargo drones into existing supply chains for postal services, retailers, and e-commerce platforms [6]. A dose of diabetes medication was autonomously delivered to the Aran Islands off the western coast of Ireland, covering a 22 km distance in just 17 min of flight time. In Scotland, two-way Beyond Visual Line of Sight (BVLOS) flights between two hospitals have significantly reduced delivery times from up to 6 h one-way by ground transport and ferry to around 15 min. Dronamics is the world's first cargo drone airline, which was officially launched in 2023 [7]. The instant logistic provider Zipline partnered

with the Ghanaian government in 2019 for the drone delivery of medical supplies. A total of 30 drones operate out of four distribution centers in Ghana to distribute vaccines, blood, and life-saving medications to 2000 health facilities across the nation daily [8]. The drone delivery company Wing, a subsidiary of Alphabet (Street Arcata, CA, USA, 2019), launched the first commercial service of delivering on-demand groceries to the general public in Virginia, Finland, and Australia [9]. In the same month, it gained the approval of the Federal Aviation Administration (FAA) Standard Part 135 air carrier certificate in October 2019. Wing's aircraft was designed to deliver small packages that weigh approximately 1.2 kg or less by lowering a tether and automatically releasing them in the desired delivery area. Skyports Drone Services and Norwegian energy firm Equinor partnered to trial electric drone deliveries by the fixed-wing "Swoop Aero Kite" to oil installations in the North Sea. The project aimed to demonstrate how on-demand cargo drone services can solve logistical challenges and improve safety and sustainability in the offshore environment. The fully electric aircraft has a 5 kg payload capacity, has a range of up to 175 km, and can operate in harsh weather conditions, including wind and rain [10].

The EU-funded AIRCARRUS project proposed an autonomous rapid response drone delivery system without ground operators for launching or retrieving operations, leveraging existing EU Commission technology programs from the Galileo GPS to the SESAR U-Space network [11]. The HL4 Herculift manufactured by the AEDRON company is a heavy lifting quadrotor of 12 kg max payload with less than 25 kg maximum takeoff weight (MTOW). The feasibility of using off-the-grid jump stations powered only by renewable green energy systems (solar/wind) to service areas with limited infrastructure was also addressed within the project. Finally, a series of large-scale demonstrations in London and Frankfurt/Main took place throughout 2022 within the framework of the EU project CORUS-XUAM. The flight tests focused particularly on the testing of deconfliction manoeuvres and speed reduction to maintain separation with commercial air traffic [12]. EuroDRONE was an unmanned traffic management (UTM) demonstration project, funded by the EU's SESAR organization, aiming to test and validate key UTM technologies for Europe's 'U-Space' UTM program [13]. Extended flights up to 10 km with Beyond Visual Line-of-Sight (BVLOS) capabilities were achieved with high levels of automation for small cargo (e.g., medical) mission operations with proven feasibility for most U-Space services). Two practical demonstrations took place in July and October 2019 at the airport of Mesolonghi in Greece. They supported the management of drone operations and included flight planning, flight approval, tracking, airspace dynamic information, and procedural interfaces with air traffic control [14]. ASSURED-UAM is a project under the CIVITAS for aviation best practices and organizational solutions in city administrative structures for Urban Air Mobility (UAM) [15]. UAM is set to revolutionize cargo transportation services in urban and suburban areas. The community acceptance level as well as its main barriers and expected benefits have been studied in Portugal and Poland [16], while similar studies on autonomous delivery robot analyses and technological and health belief factors aimed to explain consumer acceptance [17,18].

## 2.2. Work Contributions

Besides EuroDRONE, cargo-carrying air transport services in Greece are an entirely unexplored and undeveloped area of application. Due to the limited civilian use of pilotless aircraft, the UAM concept cannot be feasible unless a performance framework addressing safety, accessibility, and sustainability is established. It is pivotal to develop robust plans for operation optimization, while considering factors like flight range, relief, performance, weather conditions, collaborative interfaces with air traffic control (ATC), as well as tracking and surveillance data exchange.

The maximum flight distance and the location of a supplier's depot are the most relevant parameters that affect the serving area of the drone-delivery urban service. [19]. The results of a recent study showed that, under the appropriate flight policies, a full-coverage low-impact UAV independent system is feasible [20]. A multitrip vehicle routing

problem (MTVRP) that compensates for the limited carrying capacity by reusing drones when possible was experimentally validated by a linear energy consumption model [21]. Reducing battery weights resulted in 10% improvement compared to solutions in which each drone had its original fixed batteries, while reusing drones led to 80% less operational costs than preventing drone reuse. Besides reusing drones, research was conducted on single drones for logistics distribution for either public transportation as moving charging stations [22,23] or new infrastructures for charging stations [24–26]. Automated service points for recharge and product-reload were incorporated into a mixed-integer linear program (MILP) that minimizes travel and resource costs [27]. Sun et al. [28] added the recharging station element to “the flying sidekick problem of traveling salesman problem” (FSTSP) proposed by Murry and Chu [29]. Similar to the presented approach, specific flight routes connect with a subset of designated parking points strategically positioned throughout an urban delivery network [30]. The majority of works in the field either focus solely on flight simulations, disregard safety and regulatory compliance, or assume that cargo drones are manufactured and operate under ideal conditions. The demonstration of precision flying, in terms of altitude and flight path, over extended periods of time, in all weather conditions during both day and night periods is a critical technical requirement for cargo drone adoption [31]. Existing research on the design process of a specialized last-mile delivery drone that incorporated both mechanical and control aspects was less consistent. Moreover, a less-studied subject is the development of an infrastructure of drop boxes to automatically hand over parcels without the need for the recipient to be present for customer convenience [32]. This study extended the current literature with a data-driven performance analysis and optimal charging station distribution in a first ever explored case study in Greece. In contrast to other approaches, the proposed model for charging stations considered:

- Vertical errors of STRM DTM to reduce the likelihood of infeasible routes, ground collisions, and inaccurate deliveries.
- The choice between two package delivery mechanisms: the suspended cable system is preferred for precise locations with altitude accuracies, especially in urban and semi-urban areas, while the ultra-light box attachment is suitable for cases of excessive wind or unavailability of the customer.

### 3. Design and Computer Systems of Cargo Drone

#### 3.1. Drone Characteristics

##### 3.1.1. Structure and Performance

The prototype cargo drone is a high-grade engineering solution with a focus on a well-balanced combination of weight, endurance, speed, and stability. The aim of the design of the structure is to have the lowest possible ratio of aircraft mass to payload capacity. The chassis is designed to be structurally predictable regarding operating loads and component attachments. The manufacturing of the prototype was completed after assembling, performing the required engineering calculations (V-M diagrams for stresses and deflections), and testing under a variety of bending conditions, drag loads, and shear forces. The process led to a quadcopter equipped with four rotors and four 29×8.7-inch fixed propellers in both clockwise and counterclockwise configurations. It features a 65” robust yet lightweight frame of 5 kg that is made of carbon fiber for structural integrity without excessive bulk. It has a length of 1200 mm and a height of 600 mm. Its MTOW of 15 kg offers a substantial payload capacity of up to 10 kg. The T-motor Lift motor is responsible for providing thrust and lift to the cargo drone, and a 12S 80A Electronic Speed Controller (ESC) controls the speed and direction of the motors by regulating the power supplied to them. A high efficiency 32,000 mAh battery produces a total of 22.8 V and weighs about 4 kg. It extends the flight time to 80 min without any payload and to 72 min with a 1 kg package onboard. It is mounted on the carbon fiber tray and is fastened into a dedicated compartment at the center of the airframe body (Figure 1). The prototype typically operates at a cruise speed of 35 km /h, maintains controlled flight without losing

lift at a stall speed of 18 km /h, and is capable of a maximum speed of 70 km /h in situations where rapid transit is necessary. The drone can handle wind speeds of up to 43 km /h or 6 Beaufort without losing control. Finally, it can withstand a maximum humidity of 90%, heat of up to 40 °C, and cold environments of up to −20 °C.



**Figure 1.** Cargo drone assembling: (left) airframe body and four fixed propellers and (right) battery fastening.

### 3.1.2. Assistive Sensors

The safety of drone deliveries is paramount, especially in densely populated urban environments. The prototype comprises three satellite positioning systems: GPS with Global Navigation Satellite System, GNSS, and integrated GLONASS. The proposed combination ensures high accuracy positioning with  $\pm 1.5$  m horizontal and  $\pm 0.5$  m vertical accuracy. The 6-DoF Inertial Measurement Unit (IMU) of the ICM type plays a pivotal role in monitoring the drone's orientation, acceleration, and angular velocity. The IMU is complemented by three accelerometers, three gyroscopes, a compass, and a magnetometer. In terms of communication and data exchange, the drone features an FPV camera for real-time video transmission and remote piloting. The inclusion of BVLOS (Beyond Visual Line of Sight) 4G connectivity enables long-distance communication and control, extending the default 10 km antenna range.

### 3.1.3. Flight Control System and Communication

The autopilot is a Pixhawk 3 with a GNSS module and onboard electronics, such as the power management system and the data comms module. The flight control system relies on the open-source software architecture of PX4 for adaptability and parameter tuning. A YR16S transmitter and a compatible Sky Station YR16S receiver support 20 channels. Data transmission between the transmitter and receiver is based on Datalink technology. The antenna has a gain of 10 dBi and the range, i.e., the maximum transmission distance, was set at 10 km. This value refers to control with a controller and without the use of the integrated 4G connection. When the 4G network is activated, the range is significantly increased. The possibility of real-time image transmission via an attached camera is also supported. The operating frequency was set at 2.4 GHz, and the number of channels was 20. The frequency change is based on FHSS (Frequency Hopping Spread Spectrum) technology. Finally, the battery of the transmission and telemetry system has a capacity of more than 3000 mAh.

to achieve equivalent autonomy to the rest of the airborne system. The electrical systems that power the motor and the autopilot operate on different electrical buses for safety and redundancy. Thus, the payload has its own independent power and comms systems.

#### 3.1.4. Firmware and Ground Control Station

Firmware is critical to the safety and performance of the prototype. It is the software that runs on the drone's on-board computer platform and manages all its functions, including the following components:

- Control mechanisms of the motors, actuators, sensors, and other components that ensure its safe operation. They are referred to as the Flight Management Unit (FMU).
- Stabilization of the drone in flight by adjusting the position of the propellers and blades to maintain the desired position and altitude.
- Flight policies, i.e., rules and measures that determine how the drone will react in different situations, such as obstacle avoidance, flight behavior during bad weather conditions, flight area restrictions, etc.
- Safety mechanisms, including actions for automatic landing in case of unexpected situations, avoidance of air accidents, and protection of system data.
- Communication protocols with the operator, including flight commands, status reports, and data from sensors.

The CAN communication protocol is supported, through which the firmware recognizes the connected devices and uses them according to the needs of the ground control station. Data transmission is encrypted to protect the confidentiality and integrity of the information. The firmware incorporates an analogue-to-digital converter (ADC) to measure analogue signals, such as voltage and current, and convert them into digital data that can be processed by the ground station software computer or the autopilot. The ground control station is an interface for monitoring, mapping, and flight planning in a variety of conditions. Mission Planner by Arduino is the corresponding open-source software that is compatible with the autopilot architecture and was installed into a laptop (Figure 2).



**Figure 2.** Field setup of the ground control station, the controller, and the cargo drone.

Mission planner performs the following main functions:

- Loading of the firmware that controls the drone on the autopilot board.
- Drawing, storing, and loading autonomous missions to the autopilot by simply entering waypoints on any cartographic background.
- Downloading and analyzing in real-time mission logs generated by the autopilot.
- Monitoring the status of the drone during telemetry operation.

- Monitoring and analyzing telemetry logs after the completion of delivery missions.

The supported elevation model is the Shuttle Radar Topography Mission (SRTM) Plus (Version 3) of global 1-arcsecond (30 m) resolution. The size of the grid used when requesting terrain altitude from the ground station is by default 100 m. The typical accuracy of its Digital Terrain Model (DTM) is 10 m with a lot of local inaccuracies. Thus, terrain following is suitable for flying at altitudes of 60 m or more.

### 3.2. Safety and Regulation Specifications

The cargo drone is equipped with an air traffic avoidance system and an Automatic Dependent Surveillance-Broadcast (ADS-B) receiver to prevent collisions with other aircraft and enhance airspace awareness. The Light Detection and Ranging (LiDAR) rangefinder set provides accurate distance measurements and motion detection. The LiDAR sensor emits laser pulses in various directions, and then, it measures the time it takes for those pulses to bounce back after hitting an object. When it detects an obstacle that poses a risk of collision, the following actions can be executed in real-time: (i) adjusting the drone's altitude and pose, (ii) slowing down, and (iii) adjusting its path to continue towards the next waypoint. Finally, a 120" Ballistic Parachute weighing 0.9 kg is incorporated for emergency situations. In Greece, the Regulation General framework for flights of Unmanned Aircraft Systems (UAS), published in Government Gazette B/3152/30.9.2016, issued special permits by the HCAA/Flight Standards Division for the Specific and Certified categories. Based on SORA 2.0, Predefined Risk Assessment (PDRA) is a simplified and acceptable means of compliance (AMC) for this specific category, as it was published to the Article 11 (risk assessment) of Regulation (EU) 2019/947 [33]. If the operation falls within the scope of one of the published PDRA, it allows the applicant to quickly develop the operator manual and to obtain evidence of compliance using the PDRA table to demonstrate that the operation is safe. The highest allowable flight altitude should be established at 400 feet (FT) above ground to mitigate the risk of cargo drones interfering with low-flying aircraft, such as helicopters. To ensure that cargo drones do not inadvertently enter restricted airspace, geofencing technology can be mandated in regulations. Virtual boundaries and no-fly zones automatically prevent cargo drones from entering prohibited areas, such as Aerodrome Traffic Zones (ATZ). Within the project, many different configurations were evaluated and narrowed down to a selection of four promising configurations for PDRA. A suggested maximum payload weight of 5 kg is recommended, allowing for stable flight over about 3–8 km at roughly 18 km /h and at an altitude over 120 m.

### 3.3. Cargo Handling Mechanisms

The cargo drone incorporates two package delivery mechanisms: (i) the suspended cable system and (ii) the ultra-light box attachment (Figure 3). The quadrotor takes off from a designated launchpad with the parcel and flies to the delivery location. A wireless circuitry in the package delivery module disengages each locking mechanism automatically, using a wireless communication protocol (Figure 4). The signal is encoded with binary data (0 or 1) and transmitted on specific radio channels or frequencies at the ground control station. The typical mission of the quadrotor with a suspended load involves descending to the desired delivery altitude, hovering, ascending to a safe altitude, and flying back to the initial position. The length of the cable and its retraction mechanism ensures that the package can be lowered to the ground with precision when the cargo drone reaches the recipient. Then, the weight of the package is offloaded from the suspension means, which enables the locking mechanism to be disengaged, thereby releasing the package. The cargo drone has the capability to autonomously retract the cable once the package has been safely delivered. With the package safely in the recipient's possession, it ascends by winding the cable back onto the winch spool. The autonomous flight planner factors in the 2 min waiting for the delivery process to end before the drone returns to base. This action ensures that the cable is retrieved and does not pose a hazard to people or objects on the ground. For the box, the cargo drone hovers above the delivery location and then drops off the parcel

either from a low altitude or by landing. Safe landing requires precise altitude control, bare terrain, and landing gear deployment. For both cases, the controller automatically opens the bottom side of the ultra-light box and releases the package. Alternatively, if manual intervention is required, then the recipient can open the box. Similar to the cable system, the cargo drone should wait for two minutes for the delivery process to conclude before returning to base. Figure 4 illustrates the flow of the procedures and the mechanisms that comprise the delivery process.

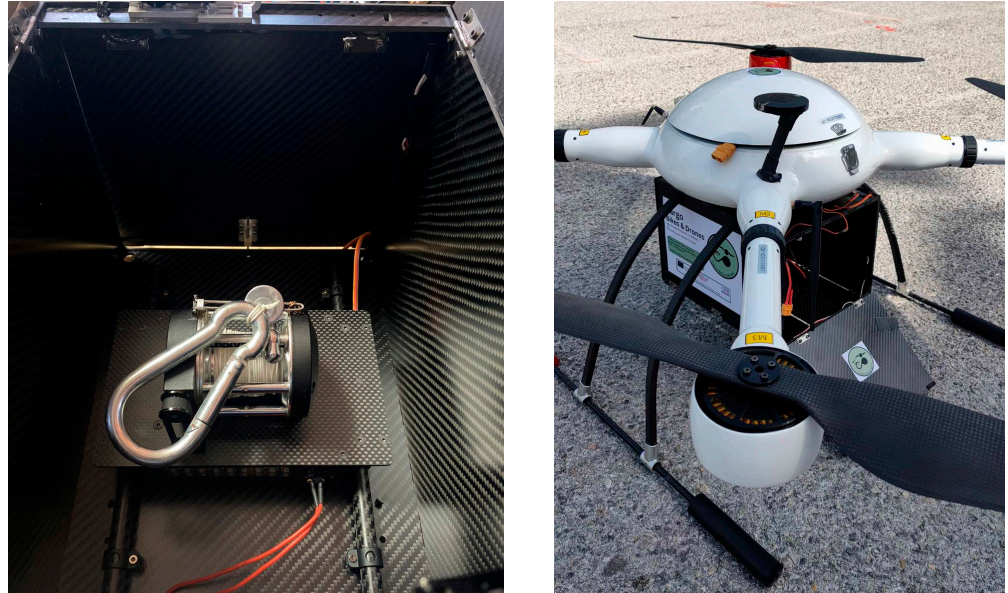


**Figure 3.** Ultra-light box with the incorporated winch mechanism.

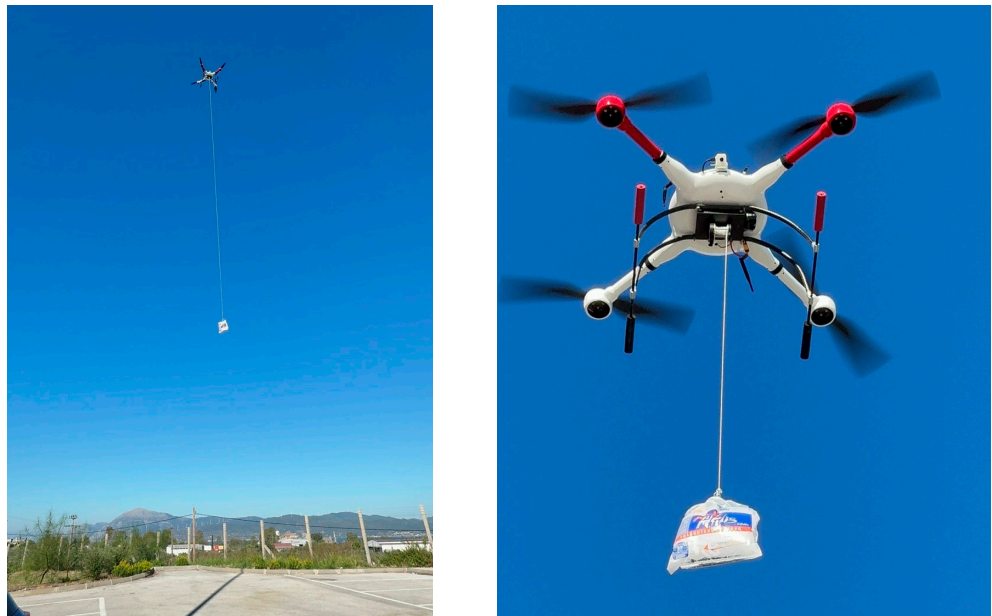


**Figure 4.** Transportation by suspending the parcel with the winch mechanism.



## 4. Methodology

### 4.1. Performance-Based Formulas

The electrical energy consumption ( $E$ ) of the battery in kilowatt-hours (kWh) associated with carrying different payload weights during cargo drone flights is given by the equation:

$$E = \frac{Ivt}{1000}, \quad (1)$$

where  $I$  is the average current drawn by the drone's motors of each flight (in Amperes),  $v$  is the average voltage supplied by the battery (in Volts) of each flight, and  $t$  is the flight duration (in hours). The linear regression model that predicts electrical energy (in mAh) based on the payload weight is expressed as follows:

$$E = \beta_0 + \beta_1 W + \varepsilon \quad (2)$$

where  $E$  is the electrical energy that the drone's battery uses (kWh) in Equation (1),  $W$  is the payload weight (kg),  $\beta_0$  is the estimated electrical energy consumption if the payload weight is zero,  $\beta_1$  is the change in electrical energy consumption for a 1 kg increase in payload weight, and  $\varepsilon$  is the error term, accounting for the variability not explained by the model, and  $\varepsilon$  is the error that accounts for variations not explained by the model. The following hypotheses were formulated:

- Null hypothesis ( $H_0$ ): there is no linear relationship between payload weight and electrical energy consumption ( $\beta_1 = 0$ ).
- Alternative hypothesis ( $H_a$ ): there is a linear relationship between payload weight and electrical energy consumption ( $\beta_1 \neq 0$ ).

The coefficient  $\beta_0$  represents the estimated energy consumption when there is no payload weight, while  $\beta_1$  represents the estimated change in energy consumption for each additional kilogram of payload weight. A positive value of  $\beta_1$  indicates that higher payload weight leads to higher energy consumption, while a negative value indicates the opposite.

Each trajectory follows a distinct route profile and speed, resulting in a significant variation in energy consumption across missions, due to the changes in flight kinematics. The typical flight profile entails vertical/horizontal motion and hovering. The total power consumption  $Ph_n$  (watts) during the phase of hovering for  $n_r$  blades is expressed as follows:

$$Ph_n = (w_d + w_k)^{3/2} \sqrt{\frac{g^3}{2\rho A_p n_r}}, \quad (3)$$

where  $w_d$  is the weight of the cargo drone, including frame, propellers, and batteries (kg);  $w_k$  is the weight of the package (kg);  $g$  is the acceleration due to gravity equal to  $9.81 \text{ m/s}^2$ ;  $\rho$  is the air density;  $A_p$  is the area of the rotor; and  $n_r$  is the number of rotor blades.

### 4.2. Altimetric Assessment

Altitude accuracy is a fundamental element of safe and effective drone operations, especially in complex urban environments with obstacles and specific altitude restrictions. Deliveries involving both landing/taking-off for the box and lowering the wire of the winch require a precise altitude to ensure that the payload is safely collected by the receiver for the intended location. Any deviation in altitude could result in the payload missing its target or being damaged during delivery. Mission Planner software integrates SRTM series 4 topography height data for setting up latitude, longitude, and height. The SRTM DEM was developed based on the images acquired by two synthetic aperture radars aboard Space Shuttle Endeavour [34]. The accuracy of the SRTM database varies over the surface of the earth. The SRTM DTED has a vertical accuracy of 16 m absolute error at 90% confidence (root-mean-square error (RMSE) of 9.73 m) world-wide. However, vertical accuracy of the data decreases with the increase in slope and elevation due to the presence of large outliers

and voids [35]. The RMSE of height differences is 6.9 m at the country level in Greece, which is 1.4 m less than the results of the tests made for the whole Eurasia region using GPS-measured points [36].

The proposed statistical measures of the height differences between the reference data and the assessed DEM are the (i) mean value  $\Delta h$  of the differences of Z coordinates of SRTM with the truth elevations of the reference and (ii) accuracy. According to the National Standard for Spatial Data Accuracy (NSSDA) of the Federal Geographic Data Committee, for a 95% level of confidence (LE95), vertical accuracy  $a$  is determined using the RMSE, as follows:

$$a = 1.96 \cdot RMSE_Z = 1.96 \sqrt{\frac{\sum (z_{data,i} - z_{ref,i})^2}{n}}, \quad (4)$$

where  $z_{data}$  is the vertical coordinate of each check point in the dataset,  $z_{ref}$  is the vertical coordinate of each check point in the independent source of higher accuracy, and  $n$  is the number of points being checked.

### 4.3. Charging Stations Distribution

#### 4.3.1. Problem Statement and Assumptions

Cargo drones are considered the only transportation fleet that handles the delivery missions entirely by pilots assigned to specific charging stations or regions. The model for extended flight range aims to determine the best charging station locations to minimize travel distance and reduce energy consumption based on the already conducted flight paths. The problem considers the possibility of recharging its battery during its route to compensate for the cargo drone's limited endurance when the minimum level of battery capacity is reached (25%). It necessitates strategic decision-making regarding the positioning and allocation of charging stations. The role of charging points is twofold: serving as refueling stations for the cargo drone and indicating weather conditions. If the charging station detects changing weather conditions during flight, such as wind speeds greater than 25 mph, temperatures below  $-10$  °C, or temperatures above 30 °C, the cargo drone should not perform the mission. Charging time at a station is 45 min to reach full battery capacity. The problem involves the set of customer locations, flight paths, and HUBs that are either the supplier's depot or open spaces where launching and landing are allowed. Increasing payload capacity may require larger batteries, affecting the overall drone weight and aerodynamics. Thus, the cargo drone can serve only one customer per dispatch. The flight request, flight plan, and flight execution from takeoff to landing are remotely piloted/automated. One flight is considered the drone transitioning from the base to the delivery location, performing the planned delivery procedures, and then flying back to the base. The developed model involves decision-making about the most suitable delivery mechanism based on real-time conditions and operational requirements. The process occurs prior to the cargo drone's flight and during its flight at the charging stations. Therefore, the decision variables of the problem define the assignment of waypoints to charging stations, the use of the winch mechanism, as well as flight times and energy consumption between locations.

#### 4.3.2. Model Formulation

The model is defined as an integer linear programming (ILP) problem aimed at finding the optimal charging station locations, while considering two primary objectives: (i) minimizing the distance for delivering packages and (ii) minimizing total electric energy consumption. Both of these involve decision-making regarding the position and allocation of charging stations. The first case aims to find the most efficient routes for the drone to cover until reaching the station, ensuring that the distance traveled is as short as possible. The second case considers battery electrical energy in terms of time for traveling between charging points, the choice of delivery mechanism, and the energy drain while the drone hovers at final locations. The battery capacity calculations for sustainable drone deliveries

are presented in Section 4.1. The waypoint  $i$  belongs to one or more flight paths  $k$  of a set of  $K$  flight paths.  $L$  is the set of HUBs where parcels are loaded and launching/landing is allowed, and  $N$  is the set of customer locations that require a package to be delivered, declared as demand points. Each waypoint  $i$  can be a potential  $j$  charging point depending on the results of the algorithm. For the first objective,  $d$  is the distance from HUB  $v$  to demand point  $n$ , and  $D_{max}$  is the maximum distance the cargo drone can travel during a single mission, including the return trip to the charging station  $j$  or the HUB  $v$ . For the second objective, the energy drain  $e(l_i, l_j, w)$  of traveling from  $l_i$  to  $l_j$  and the power consumption  $P_{h_n}$  during hovering are calculated per minute while carrying parcels of  $w$  weight. The input parameters also include the  $w$  package weights varying from 0 to 5 kg,  $u$  cargo drone speed that is equal to 5.3 m/s, and  $b$  the maximum battery capacity equal to 32,000 mAh. In order to estimate the optimal placement of charging stations on the GIS system, an extra term is introduced during the execution of the linear regression program, the coverage radius  $c_i$ . It corresponds to the radius within which a charging station can effectively cover the operational area for refueling and providing weather information. This value is then optimized to minimize the total distance and energy consumption. The operational buffer centerline  $c_i$  is less than the drone's maximum distance capacity,  $D_{max}$ . The route of the cargo drone  $k$  is completed when it departs from the HUB  $l_i$  and returns to the charging station  $j$  after covering the maximum distance depending on the weight of the parcel and the already calculated range. Finally, the position of the waypoints  $i$  that are assigned by the program to serve as charging stations  $j$  is slightly adjusted for accessibility and safety reasons. Table 1 summarizes the input parameters of the multi-object model, Table 2 shows the decision variables, and Figure 5 illustrates the charging station distribution strategy.

**Table 1.** Summary of cargo drone routing parameters and decision variables.

Input Parameters	
Name	Description
$i$	Set of waypoints.
$j$	Set of charging points.
$N = \{1, 2, \dots, n\}$	Set of demand points.
$K = \{1, 2, \dots, k\}$	Set of flight paths.
$L = \{1, 2, \dots, l\}$	Set of HUBs where launching/landing is allowed.
$w[k]$	Set of package weights, where $0 < w[k] \leq 5$ .
$d_i$	Distance from HUB to demand point $i$ , $\forall i \in N$ .
$D_{max}$	Maximum distance the cargo drone can travel during a single mission, including the return trip to the charging station or the HUB, $\forall k \in K$ .
$e(l_i, l_j, w)$	Electric energy drain per minute of traveling from $v_i$ to $v_j$ while carrying parcels of $w$ weight.
$P_h(w)$	Power consumption per minute during hovering while carrying parcels of $w$ weight.
$U$	Cargo drone speed.
$b$	Maximum energy capacity of the cargo drone's batteries.
$c$	Coverage radius of charging stations $j$ .

**Table 2.** Summary of the model's decision variables.

Decision Variables	
Name	Description
$x_{ij}$	Indicates if point $i$ is assigned to charging station $j$ , $\forall (i, j) \in N$ .
$y_j$	Indicates if the charging station $j$ is used, $\forall j \in K$ .
$z_{kj}$	Indicates the use of the winch mechanism for charging station $j$ , $\forall j \in K$ .
$t_{ij}$	Represents the time of flight from location $l_i$ to location $l_j$ while carrying parcels of $w$ weight.

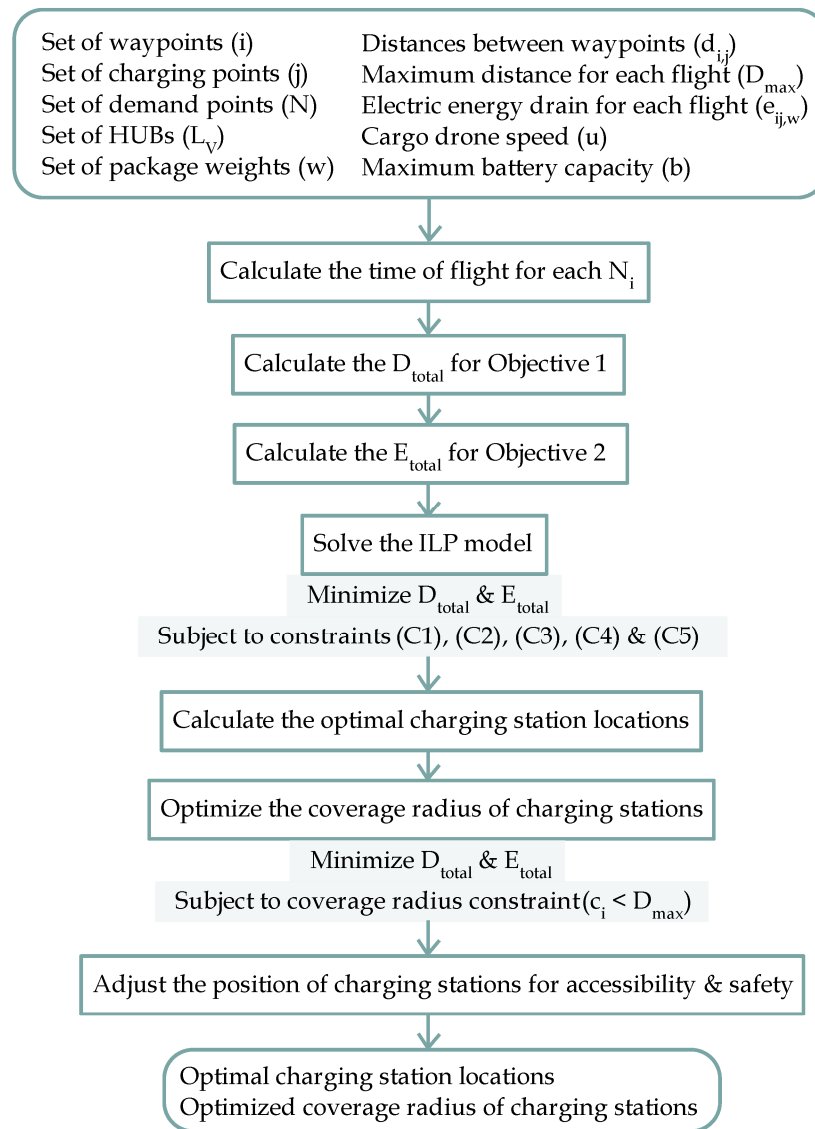


**Figure 5.** Schematic diagram of the charging station distribution problem.

Objective 1 seeks to minimize the total distance traveled by the cargo drone to deliver packages while serving each delivery point exactly once (C1). The decision variable  $x_{ij} \in [0, 1]$  indicates whether a waypoint  $i$  is assigned to charging station  $j$ , and  $y_j \in [0, 1]$  indicates whether the charging station  $j$  is used or not. The constraint (C2) enforces that each waypoint  $i$  can be assigned to only one charging station  $j$ , and the constraint (C3) restricts the maximum travel distance per flight. The variable  $z_k \in [0, 1]$  indicates the use of the winch mechanism for each flight  $k$  at the charging station  $j$ . When  $z_k$  equals 1, it signifies that the winch mechanism is in use, and this decision is guided by constraint (C4). The choice between the winch and box delivery mechanisms depends on wind conditions at the charging station.

Objective 1: Minimize the total distance:

$$\sum_{i \in N} \sum_{j \in N} d_i \cdot x_{ij}, \quad (5)$$

that is subject to the following constraints:

(C1): Each delivery point must be served exactly once:

$$\sum_{j \in N} x_{ij} = 1, \quad \forall j \in N. \quad (6)$$

(C2): Each waypoint can be assigned to only one charging station:

$$x_{ij} \leq y_j, \forall (i, j) \in N. \quad (7)$$

(C3): The maximum distance for each flight  $k$ , including the return trip:

$$2 \cdot \sum_{j \in N} d_i x_{ij} \leq D_{max} \cdot y_j. \quad (8)$$

(C4): If wind speed is greater than 25 mph at a charging station, the winch delivery mechanism is used; otherwise, the box delivery mechanism is used:

$z_{ij} = 1$  if the wind speed at the charging station is greater than 25 mph.

Objective 2 focuses on minimizing the total electrical energy consumption regarding the cargo drone's battery capacity. The decision variable  $t_{ij}$  represents the time of flight from location  $l_i$  to location  $l_j$  while carrying parcels of  $w$  weight. The total consumption does not exceed the cargo drone's battery capacity (C5). This constraint is critical for ensuring that the cargo drone operates within its energy limitations, preventing situations that could lead to mission failure or safety risks.

Objective 2: Minimize the total electric energy consumption:

$$\sum_{i \in N} \sum_{j \in N} e(l_i, l_j, w) \cdot t_{ij}, \quad (9)$$

that is subject to the same constraints of Objective 1 and, additionally, to the following one:

(C5): The total electric energy consumption is limited by the cargo drone's battery capacity  $b$  for each mission:

$$\sum_{i \in N} \sum_{j \in K} e(l_i, l_j, w) \cdot t_{ij} \leq b \cdot y_j, \forall j \in K. \quad (10)$$

## 5. Implementation

### 5.1. Flight Missions

The preliminary delivery operations mark a milestone, as cargo drone operations in Greece have been largely unexplored. They were conducted in five cities of varying geographical characteristics and logistical challenges: Athens, Iraklion, Patra, Kalamata, and Corinth. A total of 66 validation flights involved the transport of retail cargo of varying weights, using both the winch mechanism and the box. They primarily serve as benchmarks for subsequent ones through the examination of the operational capabilities of the aircraft on real scenarios and further data collection analysis. The scenarios include all necessary procedures for compliance with regulations and the safe integration of the cargo drone in the urban environment of the cities: security processes, emergency landing, recharging/maintenance, and geofencing. The flight routes were designed over the DEM of SRTM of Mission Planner and then uploaded to the cargo drone's computer system. The pilot manually launched the cargo drone with the radio control transmitter and next activated the automatic flight route, allowing it to reach the first waypoint and then fly along the provided trajectory.

Specifically, in the Regional Unit of Corinthia, a total of 12 flights were performed, covering the peri-urban and rural areas in the northern part of Corinth (Figure 6a). In the Regional Unit of Heraklion, the cargo drone executed a total of nine flights, mainly on the western and southern suburbs of the city of Heraklion. In the Regional Unit of Achaia, 12 delivery missions were performed within the urban and peri-urban areas of the city of Patras (Figure 6b). Moving to the Regional Unit of Messinia, 14 flights were conducted that primarily focused on the urban and peri-urban areas of the city of Kalamata (Figure 6c). These missions covered the eastern coastal parts of the city, including the suburbs of the town Messini and the village Petalidi. The remaining testing flights were executed within Athens, including the campus of the National Technical University of Athens and central city regions, such as Vyronas and Galatsi (Figure 7). The operations

were designed to assess the cargo drone's performance and adaptability in the densely populated metropolitan region.

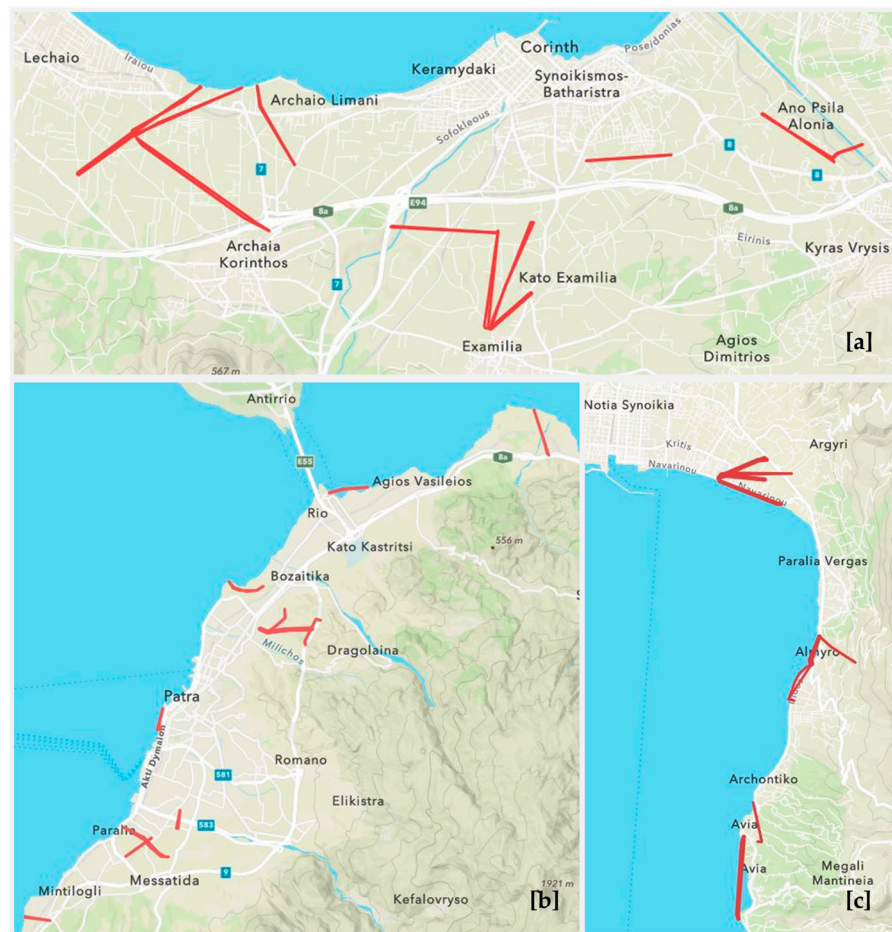


**Figure 6.** Flight routes of the cargo drone in the regional units of (a) Corinth, (b) Achaia, and (c) Messinia on the GIS system of Esri and cartographic base of Esri, METI/NASA, USGS.



**Figure 7.** Cargo drone delivering a parcel with the winch over Vyronas, Athens.

### 5.2. Data Processing

The data collected, including logfiles for each flight and on-field recordings, were stored and pre-processed using MATLAB by MathWorks [37]. Within this dataset, 49 critical variables of the telemetry logfiles were selected that align with the project's objectives. The following categories outline the variables retrieved from the different systems of the cargo drone:

- General system status: power supply, battery consumption, and system temperatures.
- Speed monitoring: rate of climb (vertical movement) and actual speed relative to the ground below, considering the drone's airspeed and the effects of wind.
- Geospatial position: the geographical position in a geocentric system derived from GPS data and sensor values.
- Attitude: the drone's orientation in relation to an aeronautical reference system, including its desired position, speed, and/or acceleration.
- Global coordinate system: the drone's position, speed, and acceleration in a global coordinate system (WGS84) and the SRTM's DEM, provided by the operator/pilot during mission planning.
- Vibrations and accelerometer clipping: vibration levels and instances of accelerometer clipping, which is a measure of abrupt changes in acceleration.

Simultaneously, information regarding weather conditions (wind speed and temperature), land use, payload weight, and the timing of the winch mechanism's operations, including suspension, descent, and elevation, were meticulously recorded in the field. Preprocessing entails several corrections and data filtering, such as the elimination of the repetitive and redundant information in the original trajectory data and the removal of zero fields and outliers. Among the 66 flights, 58 were finally used for further analysis. The excluded eight flights presented either data quality problems, such as incomplete and corrupted log files, or were nearly identical to others, offering limited additional insights.

### 5.3. Flight Range

The flight range of the cargo drone while carrying different payloads was examined for the following delivery mechanisms: (i) the box and (ii) the wire winch with the hook. They posed different challenges to cargo transportation and delivery. The box mechanism entailed landing and required less hovering time and power usage for the associated devices that release the parcel, in comparison with the winch. The modular integrated circuit of the winch consumed extra energy for de-wiring, controlling the unloading process, and pulling the wire back into the drone after delivery. Figure 8 illustrates the relationship between payload capacity, flight duration, and range using the winch and the box. The cruise speed  $u$  of the cargo drone was fixed at 5.3 m/s (19.8 km/h).

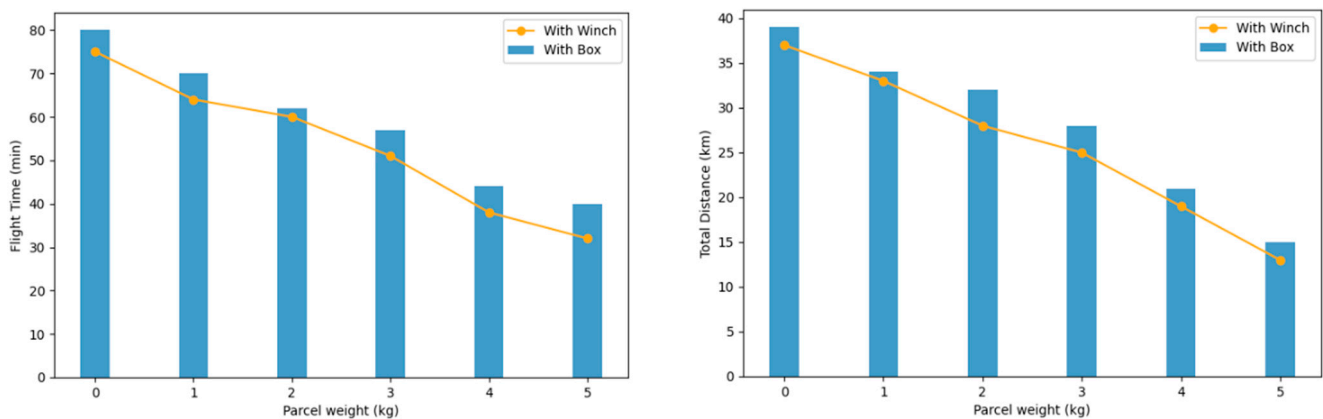


**Figure 8.** Comparison of (left) flight time and (right) total distance with winch and box delivery mechanisms for different payload weights (kg).

As was expected, the additional power consumption required to maintain flight with the larger payload resulted in a reduced operational range and flight duration. The winch mechanism consistently resulted in shorter flight times compared to the box mechanism across all payload weights. The percentage decrease in flight time compared to the box varied between 3.23% for 2 kg of parcel weight and 20% for 5 kg of parcel weight. As the payload weight increased, it added more stress and tension to the cable, causing greater oscillations and potentially making the flight less stable. It might require more energy and control efforts to counteract these vibrations, which would further reduce the efficiency of the cargo drone's operation. On the other hand, the box mechanism involved landing and taking-off for parcel release, which consumed more energy with heavier payloads. These flight modes could have contributed to the observed decrease in flight duration as payload weight increased.

## 6. Data Analysis

### 6.1. Results of Performance Evaluation

#### 6.1.1. Energy Consumption

The results of the linear regression model of Equation (2) indicated a significant linear relationship between parcel weight ( $W$ ) and electric energy consumption ( $E$ ). Table 3 shows the calculated coefficients obtained for each of the 58 flights. The flights were conducted under the same operational conditions, including takeoff weight, delivery mechanism, battery capacity (fully charged), speed, and time of hovering and waiting for the parcel to be released.

**Table 3.** Results of the energy consumption model  $\pm$  standard error  $\varepsilon$  based on the data of the flights.

Coefficients	Energy Consumption
$\beta_0$	$97.17 \pm 13.6$
$\beta_1$	$22.75 \pm 1.8$
$R^2$	0.49

The positive coefficient for parcel weight ( $\beta_1 = 22.75$ ) is a measure of how payload weight influences electric energy consumption. With a p-value less than 0.001, it suggests that an increase in parcel weight leads to a corresponding increase in energy consumption. The R-squared ( $R^2$ ) value was equal to 0.49, indicating that approximately 49% of the variance in energy consumption can be explained by parcel weight. Since the model accounted for a substantial portion of the variance in electric energy, practical implications were further examined. The flight duration and the changes of the average current that a load drew battery capacity (cA) from for every 100 g increase in parcel weight were calculated for each flight (Figure 9).

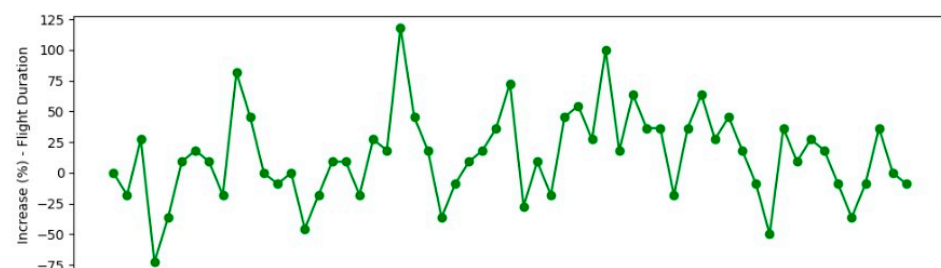


**Figure 9.** Cont.



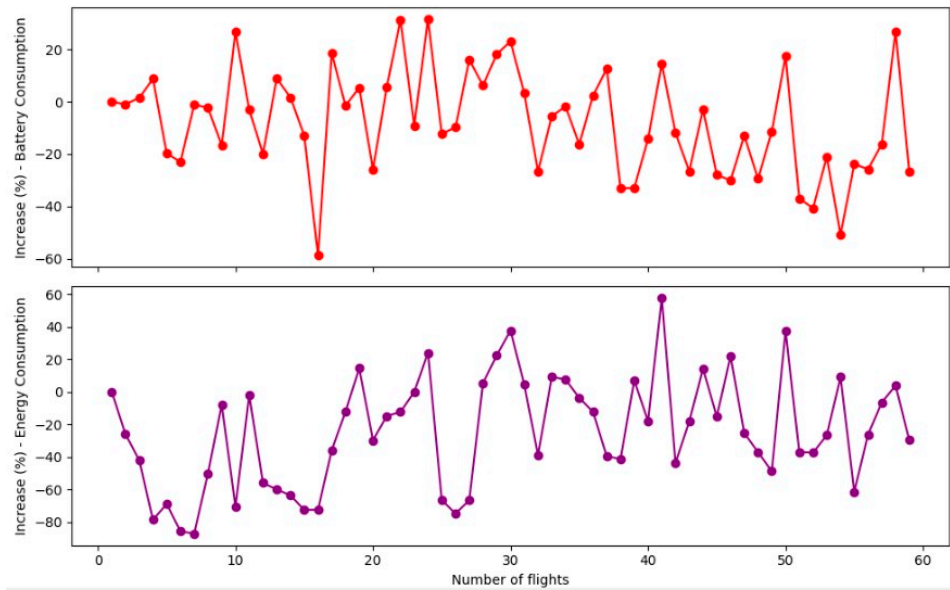


**Figure 9.** Increase (%) in flight duration (min), battery capacity (cA), and electric energy consumption (kWh) for every 100 g increase of parcel weight.

The average percentage increase in remaining battery capacity for every 100 g increase in parcel weight was approximately 3.36%. This indicates a slight positive correlation between the two of them, but the effect was relatively small. Moreover, the observed variations between battery capacity and total electric energy consumption can be attributed to external factors, such as wind speed and flight modes. The rate of electrical energy per unit wind speed (mAh/mpH) for the winch mechanism was calculated to determine if and how wind affects cargo drone’s performance (Figure 10).

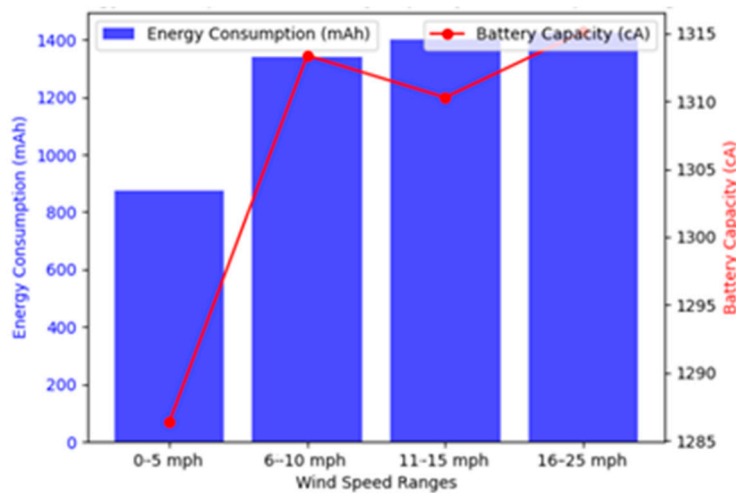


**Figure 10.** Electric energy consumption (mAh) and battery capacity (cA) for different wind speed ranges (mph).

As expected, battery usage decreased as wind speed increased. This is consistent with the reduced energy consumption rate, as cargo drones experience reduced aerodynamic drag and resistance. The onboard propulsion system (rotors, motors, etc.) did not need to adjust as frequently to compensate for gusts and changes in wind speed. In wind speed ranges of 0–5 mph and 6–10 mph, energy consumption was relatively close to the remaining battery capacity, indicating efficient energy usage. In ranges of 11–15 mph and 16–20 mph, it was noticeably lower than battery capacity, suggesting that cargo drones may have excess energy reserves in these conditions. During higher wind conditions (11–20 mph), the

cargo drone utilized the available energy more efficiently, with an average of 6.78% of energy consumption in relation to battery capacity. However, the presence of wind-induced oscillations and vibrations in the wire of the winch mechanism discouraged its use. In contrast, it is preferred in calmer wind conditions, enabling smoother and more stable flights. Different flight modes may have varying energy usage profiles. When the winch mechanism is enabled for delivery, the cargo drone hovers over the destination for 200 sec. This duration includes 80 s of descending the cable, 40 s of waiting time for parcel retrieval by the customer, and 80 s of ascending the cable. The energy consumption (Wh) during hovering for the fixed period of 200 sec was calculated for different payload weights using Equation (4) (Figure 11).

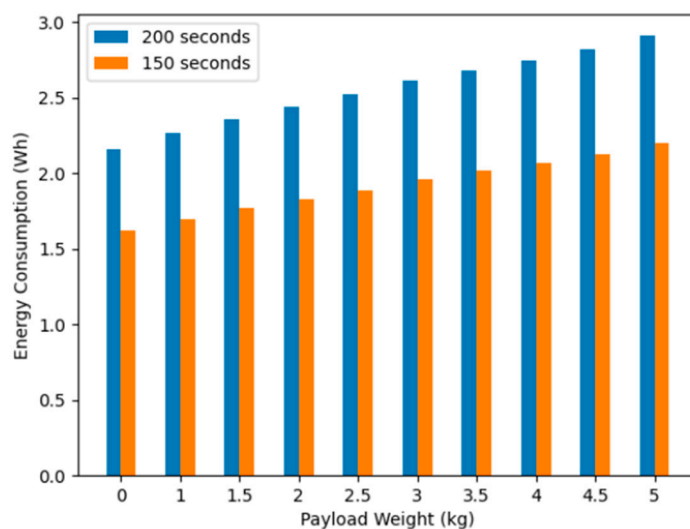


**Figure 11.** Energy consumption (Wh) during 200 sec of hovering for different payload weights (kg).

Hovering for 200 s resulted in an average of 2.55 Wh. This is a significant portion of energy considering that, for a 22.8 V battery and 2.5 kg of parcel weight, the total energy consumption was approximately 6 Wh. For lower payload weights (0 to 1.0 kg), the rate was higher (0.11 Wh/kg), and for 1.0 kg to 2.0 kg, the rate decreased slightly to 0.09 Wh/kg. It remained relatively consistent for the middle range of payload weights (1.5 kg to 4.5 kg) and increased again towards the higher ones (4.5 to 5.0 kg). A change in hovering time from 200 s to 150 s could result in average energy savings of 0.63 Wh with a standard deviation of 0.06 Wh.

#### 6.1.2. Altimetric Accuracy Assessment

The aim of this analysis was to determine the accuracy and reliability of SRTM topography height data for setting altitude in drone mission planning. The reference data for the altimetric accuracy assessment were the DEM dataset series of Hellenic Cadastre [38]. It included a 5 m pixel-size grid compilation (1:5000 cadastral tile distribution) derived from the Large Scale Orthorhotos (LSO) project, with an altimetric accuracy of 3.92 m for a 95% level of confidence. The elevation control points were the points of destination of each delivery mission, organized by Regional Unit. Figure 12 illustrates the  $\Delta h$  differences observed between the SRTM (red line) and the estimated GPS and IMU-based (blue line) altitude profile of a flight at: (a) the center of the city of Patra, (b) the foothills of Mt Ymittos in Athens, (c) the coastal part of the city of Iraklion, and (d) the rural area outside the city of Corinth. It can be observed that the steeper the terrain, the higher the uncertainty of the height of waypoints. It seems that there was a systematic offset at a regional level in the altitude measurements, except for the outlier in chart (c) around 400 s. Figure 13 correlates the  $RMSE_z$  errors of 16 check points with varying altitudes for the five case studies, which were calculated based on Equation (6). The distributions of the height differences of the SRTM exhibited relative sharpness, as indicated by the magnitude of kurtosis.

Kyrtosis characterized the relative sharpness or smoothness of a distribution, compared to the normal distribution. No correlation of the difference in altitude was observed, while more negative differences in absolute terms than positive ones (overestimation of altitude) were spotted. In general, the underestimates and overestimates of altitude were evenly distributed. The extreme negative differences (more than  $-20$  m) for Iraklion, Kalamata, and Patra were encountered for delivery destinations at sea level when the HUB was at a higher elevation. Differences exceeding  $\pm 30$  m were ignored as outliers. If the cargo drone receives a negative false elevation for its delivery destination during mission planning and relies on this while landing, it could have serious safety implications for both people and the drone itself. Assuming that it is higher above the ground than it actually is, it may descend too rapidly or too early during the landing phase. Since the error is normally distributed at the regional level in Greece, the removal of the systematic offset of around (i) 5 m for Athens and Corinth, (ii) 8 m for Kalamata, and (iii) 10 m for Patra and Iraklion prior to the mission execution is suggested for the safe conduction of flights. Cargo deliveries in coastal areas should be performed by lowering the wire of the winch at more than 30 m height. On the other hand, the high positive errors (more than 10 m) were located in areas with frequent cloud cover and high altitude. Similar to the vertical analysis for control points, the qualitative comparison of the two DEMs demonstrated that the magnitude of the error for the urban and built-up areas (land cover class 6) was similar to the values for cultivated areas.

### 6.2. Charging Stations Distribution

The goal of the proposed model was to strategically position charging stations to minimize travel distance and reduce electric energy consumption. Charging stations serve a dual purpose: refueling the drone and providing weather condition information. The decision variables involve assigning waypoints of the conducted flights to charging stations, determining the use of the winch mechanism, flight times, and energy consumption between locations. The linear regression model was solved using PuLP, which is a powerful open-source modeling package in Python [39], and the optimal position of the charging stations was visualized on ArcGIS Online [40]. Each case study exhibited unique characteristics in terms of airspace regulations, altitude variations (see Section 6.1.2), and the spatial distribution of demand points. Table 4 summarizes the results of the testing flights concerning total distance and usage of electricity of operations, the number of demand points, and the potential area of operations with no-fly zones.

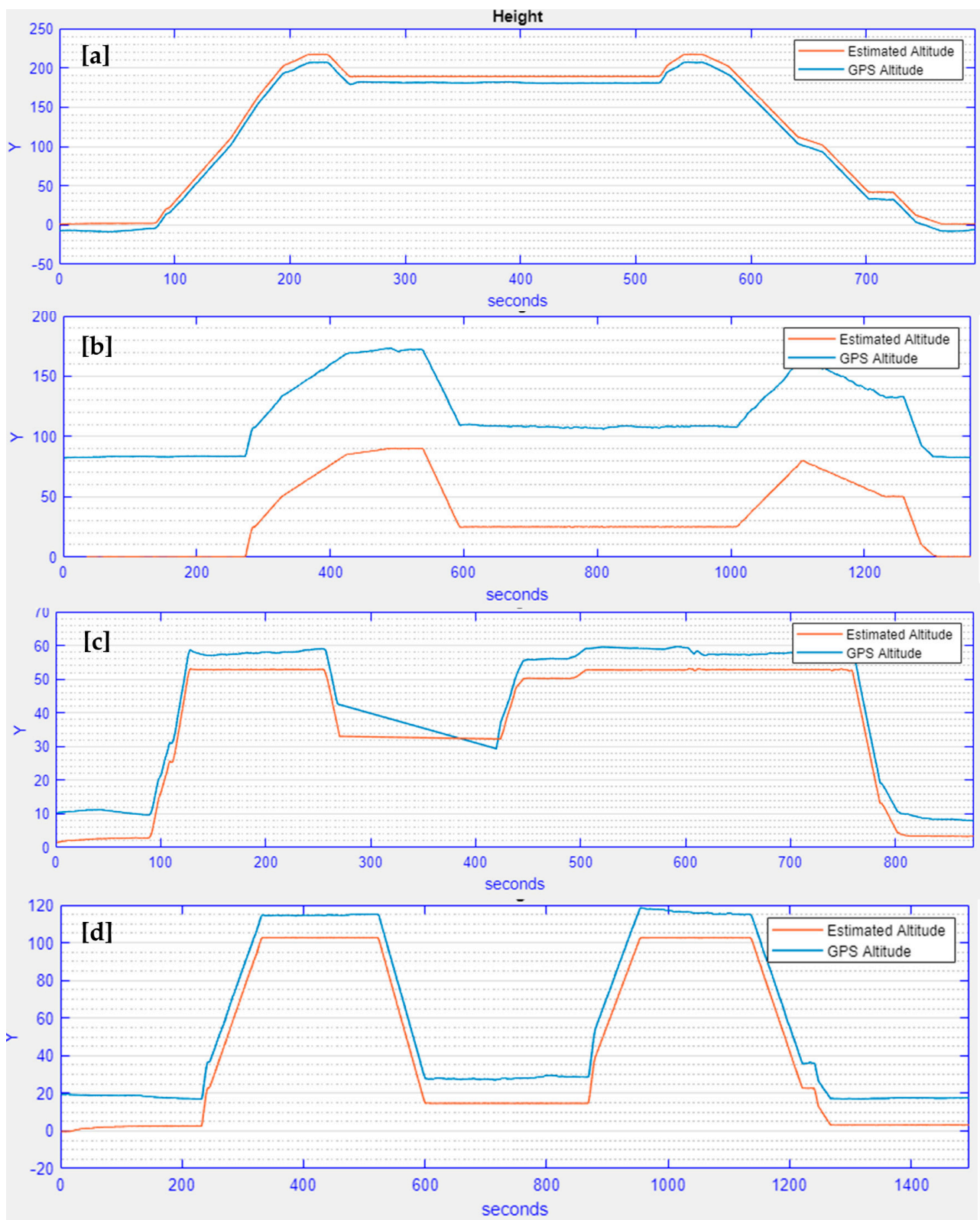


**Figure 12.** Altitude profiles (m) of trajectories of the cargo drone at: (a) the center of the city of Patra, (b) the foothills of Mt Ymittos in Athens, (c) the coastal part of the city of Iraklion using the SRTM (red line) and the estimated GPS and IMU-based (blue line) heights of waypoints, and (d) the rural area outside the city of Corinth.

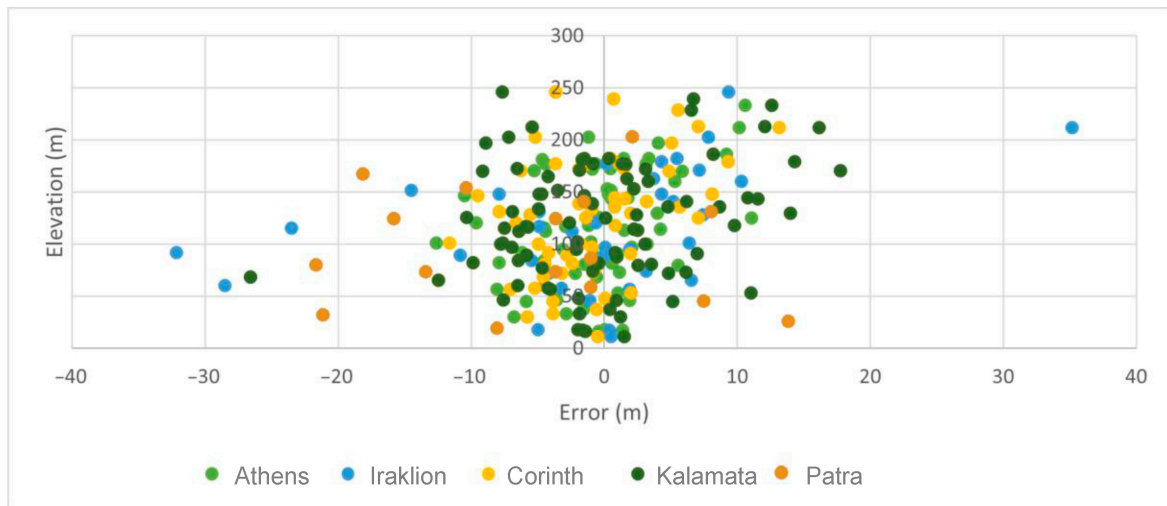


**Figure 13.** Scatter diagram of the correlation of  $RMSE_z$  errors regarding elevation for the five case studies.

**Table 4.** Total distance (km), total electric energy usage (kWh), number of demand points  $n$ , and the potential area of operations with no-fly zones ( $km^2$ ) for every case study.

Case Studies	Total Distance (km)	Total Electric Energy Consumption (kWh)	Demands Points $n$	Area with No Restrictions ( $km^2$ )
Athens	37.29	26,471.09	19	146.02
Iraklion	19.42	9929.88	9	29.33
Patra	27.03	9186.31	12	132.4
Kalamata	29.54	17,956.45	14	37.35
Corinth	35.03	9234.52	12	68.03

The model consistently showcased positive results across all cities, effectively minimizing travel distance and reducing electric energy consumption (Figure 14). Iraklion experienced the most significant reduction in travel distance (50.82%), while Patra demonstrated the highest reduction in energy consumption (46.74%). Kalamata could benefit from a 30.91% reduction in travel distance and a 41.76% reduction in energy consumption when employing the proposed charging station strategy. In Corinth, the model led to a 22.95% decrease in distance and a 29.38% decrease in energy usage, demonstrating positive outcomes for both objectives. Figure 15 illustrates the final optimal locations of charging stations in Corinth, Patra, Kalamata, and Iraklion. The complex urban layout of Athens and the absence of open spaces minimized the number of the charging stations that were initially proposed by the model (Figure 16). Thus, the charging station placement resulted in an 18.16% reduction in travel distance and a 26.25% reduction in energy consumption compared to the initial total values.

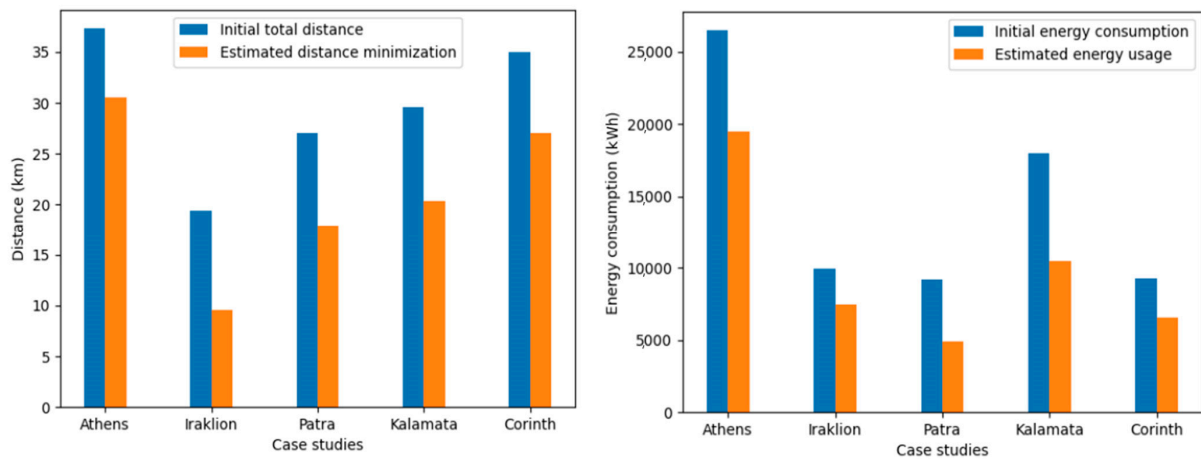


**Figure 14.** Estimated distance and electric energy usage minimization after installing charging stations based on delivering the same number and weight of parcels.

Drone deliveries should complement rather than replace existing delivery networks. To achieve this seamless integration into the urban supply chain, collaboration and partnerships with couriers and postal services are suggested. The strategically placed centralized HUBS, landing zones, and charging stations in densely populated areas can expand the reach and accessibility of deliveries of logistics providers and facilitate the handover of packages to ground transportation. Finally, the decision between dropping the package from the box and using the winch is determined by the weather conditions, the altitude of the delivery location along with the SRTM's DEM accuracy, as well as the recipient availability at the delivery location. The suspended cable system is preferred when delivering to locations with steep terrain (slope > 35% or 45 degrees), as it allows for the controlled lowering of the package. It is also particularly suggested for coastal areas where negative elevation errors are encountered, indicating a potential false elevation. On the other hand, it is less susceptible to wind. Wind invokes turbulence and sways the cable of the winch mechanism, making it challenging to precisely lower and raise packages. The box mechanism necessitates landing, which would increase the risk of collision with the ground. It is preferred in areas with flat or gently sloping terrain and in cases where the HUB and demand points have similar altitudes for vertical error mitigation. The decision also depends on whether the recipient is available at the demand point. If recipient availability is uncertain or not guaranteed and the conditions for landing are not addressed, then an automatic drop-off from a low height using the box mechanism is a practical and efficient solution.

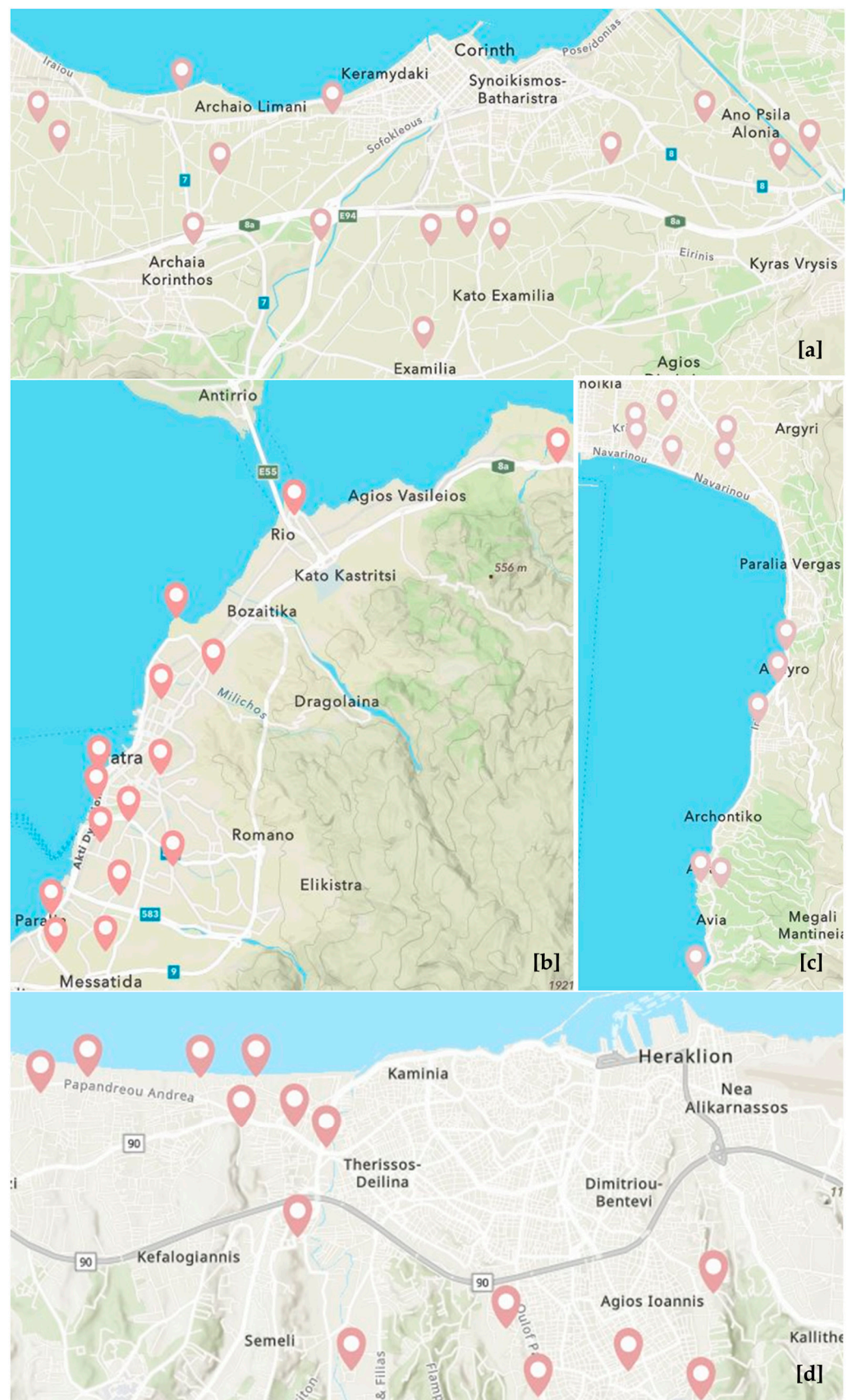


**Figure 15.** Estimated locations of charging stations in (a) Corinth, (b) Patra, (c) Kalamata, and (d) Iraklion on the GIS system of ArcGIS Online.

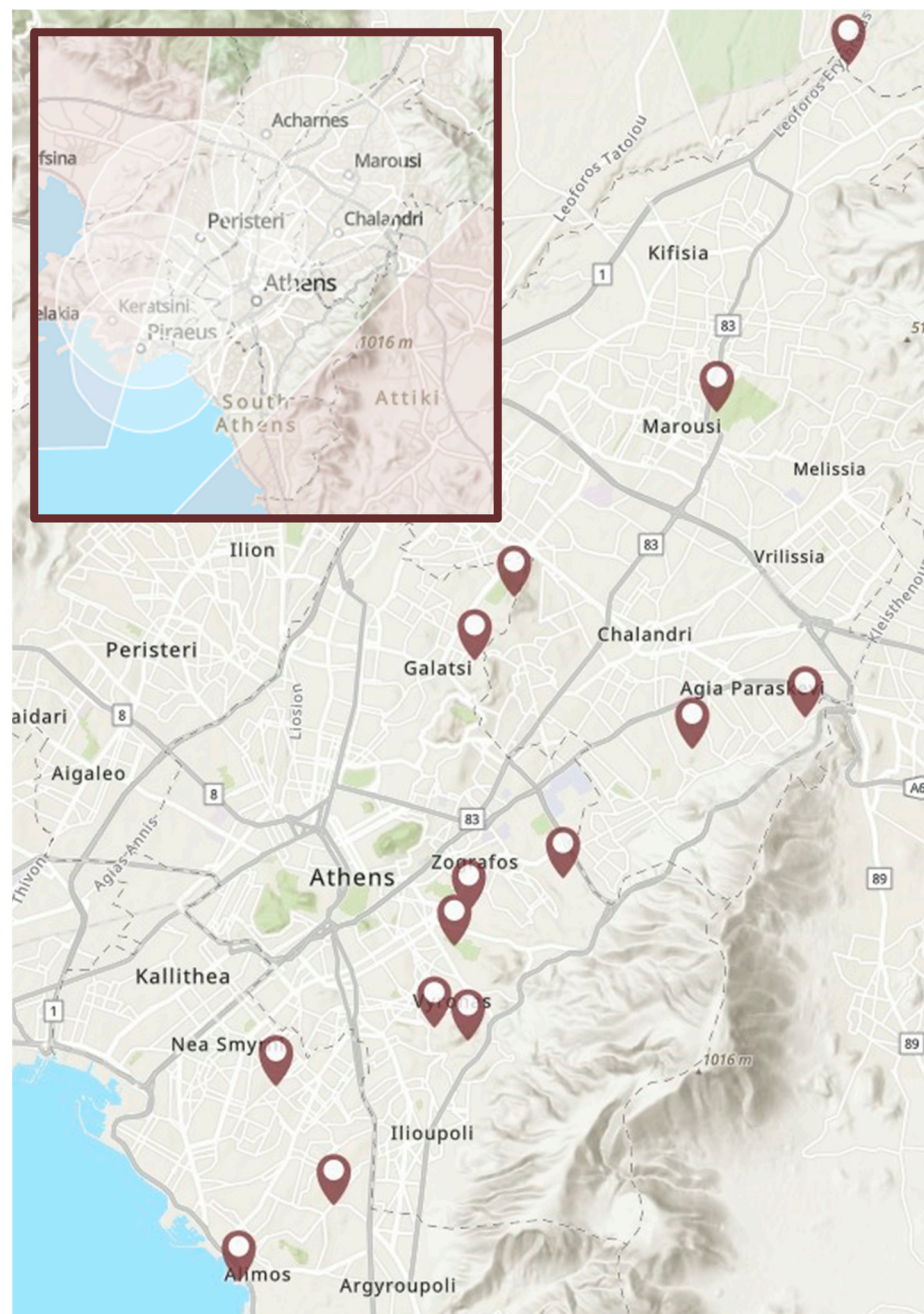


**Figure 16.** Estimated locations of charging stations in Athens and an overview of the no-fly (pink) and restricted (white) zones on the GIS system of ArcGIS Online.

### 6.3. Environmental and Economic Impact

The environmental and economic impact of cargo drone deliveries compared to traditional road transportation is based on two common metrics: carbon dioxide CO<sub>2</sub> emissions and cost per unit of distance. In this analysis, it was assumed that the 58 deliveries performed by the cargo drone missions were replicated using a diesel van employed by logistics companies, following the same routes on the existing road infrastructure to reach the same destination points. The calculated values include carbon dioxide emissions (134 g/km), minimum fuel consumption (4.4 L per 100 km), maximum fuel consumption (5.8 L per 100 km), and minimum fuel cost (EUR 1.774 /liter, average price as of 30 October 2023) (Figure 17).



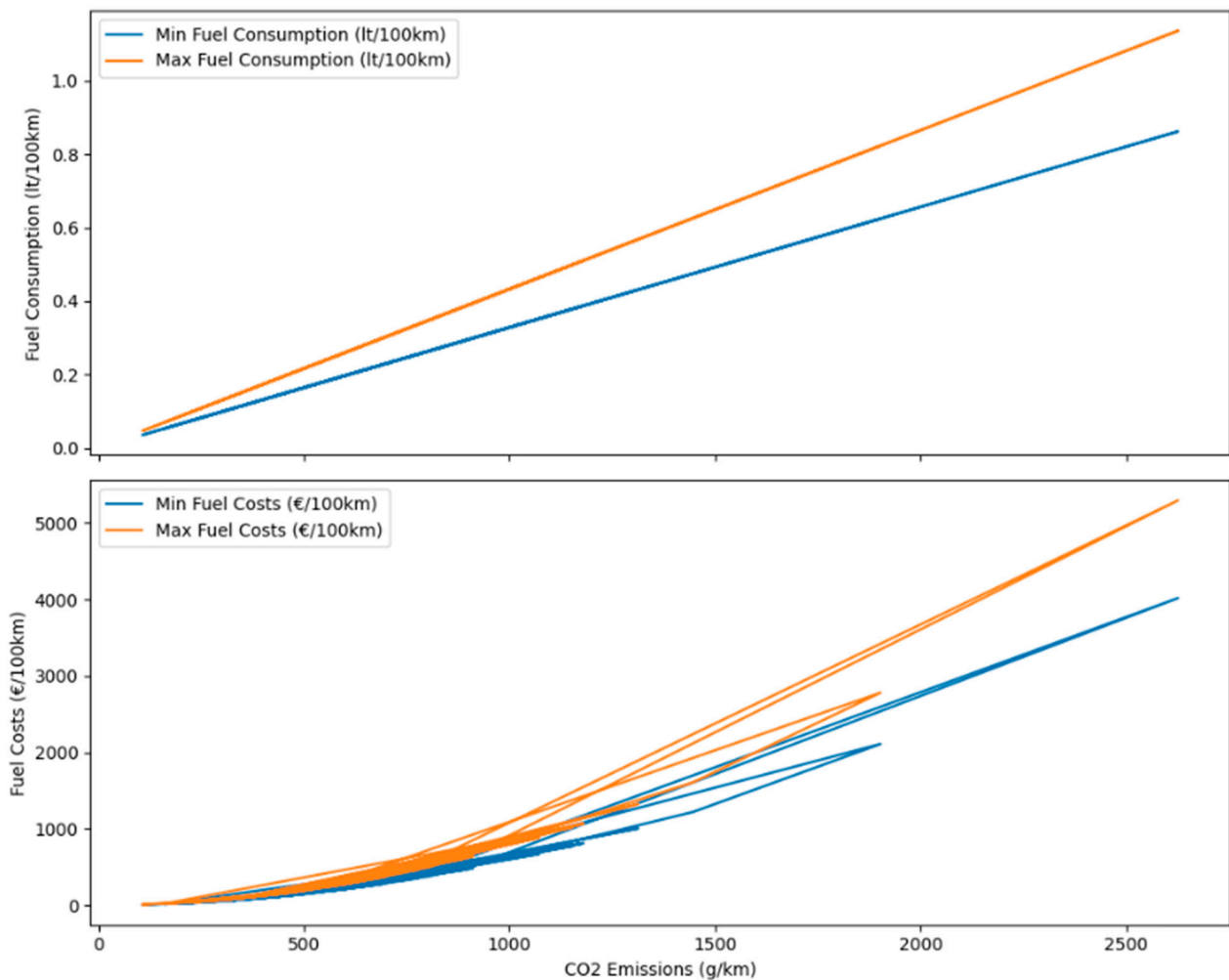


**Figure 17.** Fuel consumption (l t/100 km ) and fuel costs (EUR/100 km ) based on CO<sub>2</sub> emissions for the corresponding delivery missions using a diesel van.

The environmental impact of the cargo drone is associated with the capacity and voltage of its battery, as well as with the charging time. In the case of a battery with a capacity of 32,000 mAh and a voltage of 22.8 V, with a 45 min charging duration, the energy usage amounted to 0.547 kWh. Each charge costs EUR 0.0547 based on the electricity price in Greece, which is EUR 0.1 per kWh. The carbon emissions depend on the carbon intensity of the electricity used for charging. The carbon intensity in Greece in 2022 was 344 gCO<sub>2</sub>/KWh, resulting in 187.2 g of emissions per charge. The transportation of a parcel of 3 kg using the box delivery mechanism corresponded to an operational range of 28 km before recharging, which is equivalent to 6.686 g/km CO<sub>2</sub> emissions and EUR 0.001/km cost. Table 5 presents the comparison between the environmental footprint (g/km) and the operational cost (EUR/km) between the cargo drone and the conventional truck derived from the statistical analysis of the total of 58 data flights.

The cargo drone demonstrated a significant reduction in CO<sub>2</sub> emissions per kilometer compared to the truck, with reductions ranging from 50.18% to 77.42%. The median emissions for the cargo drone (200.58 g/km) were also substantially lower than the truck's median emissions (559.60 g/km), indicating a 64.10% reduction in the carbon footprint. The drone had a lower standard deviation (64.79 g/km) compared to the truck (425.43 g/km). Regarding operational costs, cargo drone deliveries are a more cost-effective option for short-distance transport when compared to conventional road transportation. Even the minimum cost for the cargo drone (EUR 0.015/km) is lower than the truck's minimum cost (EUR 0.087/km), indicating a minimum reduction of 82.76%. It must be noted that the

maximum payload and range of the cargo drone restricts the weight, volume, and number of parcels being delivered compared to the quantity of items that can be transported using trucks. Moreover, compliance with local airspace regulations may require the drone to take longer flight distances or detours to avoid restricted areas. This would necessitate more power for propulsion and may lead to higher CO<sub>2</sub> emissions if the energy source is not entirely clean or renewable.

**Table 5.** Statistics of the CO<sub>2</sub> emissions (g/km) and operational cost (EUR/km) for the cargo drone and a conventional delivery truck, covering the same distances.

	Cargo Drone		Truck	
	CO <sub>2</sub> Emissions (kg/km)	Operational Cost (EUR/km)	CO <sub>2</sub> Emissions (kg/km)	Operational Cost (EUR/km)
Mean	0.18627	0.028	0.6609	1.179
Median (50th percentile)	0.20058	0.030	0.4556	0.343
Standard deviation	0.64789	0.007	0.3455	2.342
Minimum	0.10029	0.015	0.1608	0.062
Maximum	0.26075	0.039	1.9028	11.083

## 7. Conclusions

The presented work aimed to provide valuable insights into the complex dynamics of cargo drone operations, assessing its performance and offering practical guidance for the ongoing development and deployment of these innovative aerial delivery solutions in Greece. The design and construction of a tailored-to-last mile logistics drone facilitated hands-on experimentation and data collection, reinforcing the empirical validation of a charging station distribution problem. By subjecting it to varying conditions during 58 delivery cases in Athens, Iraklion, Patra, Kalamata, and Corinth, empirical data that reflected its real-world performance under different operational constraints were gathered, processed, and analyzed. The cargo drone's performance was notably affected by the payload, while there was a slight positive correlation between parcel weight and remaining battery capacity, with an average increase of approximately 3.36% for every 100 g increase in parcel weight. It had significantly lower operational costs on average compared to the truck, with an estimated reduction of approximately 89.44%. Its maximum emissions (260.75 g/km) were considerably lower than the truck's maximum emissions (1152.40 g/km), representing a maximum reduction of 77.42%.

The cargo drone integrated both a box and a winch delivery mechanism. The winch mechanism can reach destination points of steep terrain and high altitude due to the controlled loading/unloading of the wire where the parcel is suspended. Extreme negative differences in altitude (more than −20 m) in coastal areas of the SRTM elevation model of the Mission Planner software emphasized the need to consider safety implications, suggesting that cargo deliveries in such areas should be performed by lowering the winch wire at more than 30 m height. However, the winch is discouraged in wind-induced oscillations and vibrations, making it less favorable in turbulent conditions. Hovering above the destination location corresponds to 42.5% of the average energy consumption. Therefore, a change in hovering time from 200 s to 150 s results in average energy savings of 0.63 Wh. The box mechanism is more suitable for scenarios where landing and taking off consume relatively less energy compared to the added stability benefits.

The findings from these scenarios provide valuable insights into the practicality and viability of utilizing cargo drones in urban and peri-urban environments. The proposed model for installing and strategically positioning charging stations aligns with the goals of minimizing travel distance and energy consumption for sustainable drone deliveries. It can serve as a basis for further research and development on customer-centric drone delivery in Greece, corresponding model formulations, solution algorithms, and potential comparisons of the performance of various alternative system designs. The overall rate

of reduction for distance across the five case studies was approximately 41.03%, and for energy consumption, it was approximately 56.73%. Moreover, the developed decision-making algorithm enabled the cargo drone to choose the appropriate delivery mechanism depending on wind conditions, terrain profiling, and flight range. Readily accessible charging infrastructure creates the potential for longer routes and a higher volume of deliveries within a given timeframe. To reduce the overall environmental impact and to ensure continuous and eco-friendly energy supply, they may be powered by renewable energy sources, such as solar panels.

Further optimization of the charging station network should be explored, considering factors beyond distance and energy consumption. Integrating real-time traffic data, delivery demand patterns, and urban development plans may lead to a more robust model for their strategic placement. Quantifying cost savings or examining the value of the improvements in performance, such as the reduction in delivery times or the increase in customer satisfaction, are crucial steps for future endeavors. Alternative routing algorithms, different charging station configurations, or even combined delivery methods, such as cargo bikes, ground vehicles, or human couriers, could be integrated into the proposed model and tested. Future works might also refine the decision-making algorithm to dynamically adjust delivery mechanisms based on real-time weather data, such as wind direction, temperature, and air density.

Given that cargo drone logistics remain unexplored in Greece, cargo drones may find their niche in specific-use cases, such as delivering medical supplies to remote areas or time-sensitive goods to congested urban environments. Their integration into last-mile supply requires a coordinated effort from government bodies, industry stakeholders, and the public. Key challenges need to be tackled, comprising air traffic control, compliance with airspace regulations, safety of people and property, and potential noise pollution. Gaining public acceptance is the last and most significant step toward the successful integration of drones. Cargo drones will be embraced if people and regulation authorities understand the benefits and if they trust and witness them in action under real-world conditions. Thus, extensive piloted flights play a crucial role in showcasing their efficiency, reliability, and cost-effectiveness.

**Author Contributions:** Conceptualization, C.P., C.I. and S.S.; methodology, C.P., A.-M.B. and G.T.; software, A.-M.B. and G.T.; validation, C.P., C.I. and S.S.; formal analysis, S.S.; investigation, R.C. and G.T.; resources, A.-M.B., G.T. and R.C.; data curation, G.T. and R.C.; writing—original draft preparation, A.-M.B., C.P. and S.S.; writing—review and editing, C.P., C.I. and A.-M.B.; visualization, S.S., A.-M.B. and G.T.; supervision, C.P. and C.I.; project administration, C.I. All authors have read and agreed to the published version of the manuscript.

**Funding:** This research was co-financed by the European Regional Development Fund of the European Union and Greek national funds through the Operational Program Competitiveness, Entrepreneurship, and Innovation, under the call RESEARCH—CREATE—INNOVATE (project code: T2EΔK-04829).

**Data Availability Statement:** The data presented in this study are available upon request from the corresponding author.

**Acknowledgments:** Giannis Koutsoulas of the company “Greekrotors” contributed to the assembly of the prototype cargo drone and the flying missions.

**Conflicts of Interest:** The authors declare no conflict of interest.

## References

1. Advance Notice of Proposed Amendment 2015-10, EASA. Available online: <https://www.easa.europa.eu/sites/default/files/dfu/A-NPA%202015-10.pdf> (accessed on 30 October 2023).
2. OpenTopography Shuttle Radar Topography Mission (SRTM) Global. 2013. Available online: <https://portal.opentopography.org/dataset/Metadata?otCollectionID=OT.042013.4326.1> (accessed on 30 October 2023).
3. ArduPilot Dev Team. Mission Planner. Available online: <https://ardupilot.org/planner/> (accessed on 30 October 2023).
4. Amazon. Amazon Prime Air. Available online: <https://goo.gl/CScVNp> (accessed on 30 October 2023).

5. Jung, S.; Kim, H. Analysis of Amazon Prime Air UAV Delivery Service. *J. Knowl. Inf. Technol. Syst.* **2017**, *12*, 253–266.
6. Wingcopter. Available online: <https://wingcopter.com/> (accessed on 30 October 2023).
7. Dronamics. Available online: <https://www.dronamics.com/> (accessed on 30 October 2023).
8. Healthcare MEA. Zipline Expands Medical Drone Deliveries in Ghana. *HealthCare Middle East & Africa Magazine*. Available online: <https://www.healthcaremea.com/zipline-expands-medical-drone-deliveries-in-ghana/> (accessed on 30 October 2023).
9. Porter, J. Alphabet's Nascent Drone Delivery Service Is Booming. *The Verge*. Available online: <https://www.theverge.com/2020/4/9/21214709/alphabet-wing-drone-delivery-coronavirus-covid-19-demand-increase-toilet-paper-baby-food> (accessed on 30 October 2023).
10. Skyports Drone Services. Available online: <https://skyportsdroneservices.com/skyports-drone-services-partners-with-equinor-for-cargo-drone-deliveries-to-offshore-oil-field/> (accessed on 30 October 2023).
11. AIRCARRUS—Autonomous Drone Delivery System. Available online: <https://cordis.europa.eu/article/id/415490-building-the-world-s-drone-infrastructure/> (accessed on 30 October 2023).
12. CORUS-XUAM. Available online: <https://corus-xuam.eu/> (accessed on 30 October 2023).
13. Lappas, V.; Zoumponos, G.; Kostopoulos, V.; Lee, H.I.; Shin, H.-S.; Tsourdos, A.; Tantardini, M.; Shomko, D.; Munoz, J.; Amoratis, E.; et al. EuroDRONE, a European Unmanned Traffic Management Testbed for U-Space. *Drones* **2022**, *6*, 53. [CrossRef]
14. SES Area Member States, U-Space Services, Implementation Monitoring Report. Available online: <https://www.eurocontrol.int/sites/default/files/2020-09/ospace-services-implementation-monitoring-report-2020-1-1.pdf> (accessed on 30 October 2023).
15. Silva, A.T.; Duarte, S.P.; Melo, S.; Witkowska-Konieczny, A.; Giannuzzi, M.; Lobo, A. Attitudes towards Urban Air Mobility for E-Commerce Deliveries: An Exploratory Survey Comparing European Regions. *Aerospace* **2023**, *10*, 536. [CrossRef]
16. Thipphavong, D.P.; Apaza, R.; Barmore, B.; Battiste, V.; Burian, B.; Dao, Q.; Feary, M.; Go, S.; Goodrich, K.H.; Homola, J.; et al. Urban Air Mobility Airspace Integration Concepts and Considerations. In Proceedings of the 2018 Aviation Technology, Integration, and Operations Conference, Atlanta, GA, USA, 24–28 June 2018; American Institute of Aeronautics and Astronautics: Atlanta, GA, USA, 2018.
17. Yuen, K.F.; Cai, L.; Lim, Y.G.; Wang, X. Consumer Acceptance of Autonomous Delivery Robots for Last-Mile Delivery: Technological and Health Perspectives. *Front. Psychol.* **2022**, *13*, 953370. [CrossRef] [PubMed]
18. Arntz, E.M.; Van Duin, J.H.R.; Van Binsbergen, A.J.; Tavasszy, L.A.; Klein, T. Assessment of Readiness of a Traffic Environment for Autonomous Delivery Robots. *Front. Future Transp.* **2023**, *4*, 1102302. [CrossRef]
19. Sawadsitang, S.; Niyato, D.; Tan, P.S.; Wang, P. Supplier Cooperation in Drone Delivery. In Proceedings of the 2018 IEEE 88th Vehicular Technology Conference (VTC-Fall), Chicago, IL, USA, 27–30 August 2018; IEEE: Chicago, IL, USA, 2018; pp. 1–5.
20. ElSayed, M.; Foda, A.; Mohamed, M. The Impact of Civil Airspace Policies on the Viability of Adopting Autonomous Unmanned Aerial Vehicles in Last-Mile Applications. *Transp. Policy* **2024**, *145*, 37–54. [CrossRef]
21. Dorling, K.; Heinrichs, J.; Messier, G.G.; Magierowski, S. Vehicle Routing Problems for Drone Delivery. *IEEE Trans. Syst. Man Cybern. Syst.* **2017**, *47*, 70–85. [CrossRef]
22. Huang, H.; Savkin, A.V.; Member, S.; Huang, C. Round trip routing for energy-efficient drone delivery based on a public transportation network. *IEEE Trans. Transp. Electr.* **2020**, *6*, 1368–1376. [CrossRef]
23. Moadab, A.; Farajzadeh, F.; Fatahi Valilai, O. Drone Routing Problem Model for Last-Mile Delivery Using the Public Transportation Capacity as Moving Charging Stations. *Sci. Rep.* **2022**, *12*, 6361. [CrossRef] [PubMed]
24. Hong, I.; Kuby, M.; Murray, A.T. A range-restricted recharging station coverage model for drone delivery service planning. *Transp. Res. Part C Emerg. Technol.* **2018**, *90*, 198–212. [CrossRef]
25. Gan, X.; Zhang, H.; Hang, G.; Qin, Z.; Jin, H. Fast-charging station deployment considering elastic demand. *IEEE Trans. Transp. Electr.* **2020**, *6*, 158–169. [CrossRef]
26. Huang, H.; Savkin, A.V. A method of optimized deployment of charging stations for drone delivery. *IEEE Trans. Transp. Electr.* **2020**, *6*, 510–518. [CrossRef]
27. Kim, J.; Morrison, J.R. On the Concerted Design and Scheduling of Multiple Resources for Persistent UAV Operations. *J. Intell. Robot Syst.* **2014**, *74*, 479–498. [CrossRef]
28. Sun, D.; Peng, X.; Qiu, R.; Huang, Y. The traveling salesman problem: Route planning of recharging station-assisted drone delivery. In Proceedings of the Fourteenth International Conference on Management Science and Engineering Management, Toledo, Spain, 1–4 August 2021; Springer: Berlin/Heidelberg, Germany, 2021; Volume 2, pp. 13–23.
29. Murray, C.C.; Chu, A.G. The flying sidekick traveling salesman problem: Optimization of drone-assisted parcel delivery. *Transp. Res. Part C Emerg. Technol.* **2015**, *54*, 86–109. [CrossRef]
30. Rave, A.; Fontaine, P.; Kuhn, H. Drone Location and Vehicle Fleet Planning with Trucks and Aerial Drones. *Eur. J. Oper. Res.* **2023**, *308*, 113–130. [CrossRef]
31. Mohammed, F.; Idries, A.; Mohamed, N.; Al-Jaroodi, J.; Jawhar, I. UAVs for Smart Cities: Opportunities and Challenges. In Proceedings of the 2014 International Conference on Unmanned Aircraft Systems (ICUAS), Orlando, FL, USA, 27–30 May 2014; IEEE: Orlando, FL, USA, 2014; pp. 267–273.
32. Li, F.; Kunze, O. A Comparative Review of Air Drones (UAVs) and Delivery Bots (SUGVs) for Automated Last Mile Home Delivery. *Logistics* **2023**, *7*, 21. [CrossRef]

33. Rauhala, A.; Tuomela, A.; Leviäkangas, P. An Overview of Unmanned Aircraft Systems (UAS) Governance and Regulatory Frameworks in the European Union (EU). In *Unmanned Aerial Systems in Agriculture*; Elsevier: Amsterdam, The Netherlands, 2023; pp. 269–285.
34. Rabus, B.; Eineder, M.; Roth, A.; Bamler, R. The shuttle radar topography mission—A new class of digital elevation models acquired by spaceborne radar. *ISPRS J. Photogramm. Remote Sens.* **2003**, *57*, 241–262. [[CrossRef](#)]
35. NASA. The Shuttle Radar Topography Mission (SRTM) Collection User Guide. Available online: [https://lpdaac.usgs.gov/documents/179/SRTM\\_User\\_Guide\\_V3.pdf](https://lpdaac.usgs.gov/documents/179/SRTM_User_Guide_V3.pdf) (accessed on 30 October 2023).
36. Ioannidis, C.; Xinogalas, E.; Soile, S. Assessment of the Global Digital Elevation Models ASTER and SRTM in Greece. *Surv. Rev.* **2014**, *46*, 342–354. [[CrossRef](#)]
37. *MATLAB*, 9.13.0 (R2022b); The MathWorks, Inc.: Natick, MA, USA, 2022. Available online: <https://www.mathworks.com> (accessed on 30 October 2023).
38. Digital Elevation Model—DEM—LSO Project, Hellenic Cadastre. Available online: <https://gis.ktimanet.gr/geoportal/catalog/search/resource/details.page?uuid=%7B456CB655-B899-450A-87BF-8322B8FB8370%7D> (accessed on 30 October 2023).
39. PuLP, A Python Linear Programming API. Available online: <https://github.com/coin-or/PuLP> (accessed on 30 October 2023).
40. ArcGIS Online, ESRI. Available online: <https://www.arcgis.com/index.html> (accessed on 30 October 2023).

**Disclaimer/Publisher’s Note:** The statements, opinions and data contained in all publications are solely those of the individual author(s) and contributor(s) and not of MDPI and/or the editor(s). MDPI and/or the editor(s) disclaim responsibility for any injury to people or property resulting from any ideas, methods, instructions or products referred to in the content.